

MR Cholangiopancreatography (MRCP)

Thomas G. Vrachliotis,¹ Ali Shirkhoda,* Kostaki G. Bis, Anil N. Shetty, Orhan Konez,² John J. Ference, and Beatrice L. Madrazo

Department of Diagnostic Radiology, William Beaumont Hospital, Royal Oak, MI 48073

¹Current address: Ohio State University Medical Center, Department of Radiology, Rhodes Hall, 450 W. 10th Avenue, Columbus, OH 43210; ²Current address: Aultman Hospital, Department of Radiology, 2600 6th Street, SW., Canton, OH 44710

* Address correspondence to: Ali Shirkhoda, M.D., Department of Diagnostic Radiology, William Beaumont Hospital, Royal Oak, MI 48073. Telephone #: (810) 551-1004; Fax #: (810) 551-3521

ABSTRACT: Magnetic resonance cholangiopancreatography (MRCP) is an evolving new technique for noninvasive imaging of diseases of the biliary tree and pancreatic duct. The advantage of this method is that one can obtain maximum intensity projection (MIP) images of the pancreatobiliary system similar to those obtained with endoscopic retrograde cholangiopancreatography (ERCP) without the need of administration of intravenous or oral contrast. Heavily T2-weighted sequences are used that render the bile and the intraductal pancreatic fluid bright against a dark background.¹

KEY WORDS: magnetic resonance cholangiopancreatography (MRCP), noninvasive imaging, biliary tree, pancreatic duct.

I. EVOLUTION OF MRCP

Within the last 5 years, MRCP has rapidly developed to the point that it is clinically used in many institutions. A breath hold T2-weighted 2D gradient echo sequence using steady state free precession (SSFP) was first described by Wallner et al.² Coronal images of the biliary tree resembling those of percutaneous transhepatic cholangiography (PTC) and endoscopic retrograde cholangiopancreatography (ERCP) were obtained. In their study, 13 patients with obstructive jaundice were studied, and the cause of jaundice was determined in 8 of the 13 cases. Subsequently, Morimoto et al.,³ Ishizieki et al.,⁴ and Hall-Craggs et al.,⁵ also using GRE techniques with SSFP, reported good correlation between MRCP findings and those from direct cholangiography. The limitations of those techniques were due to field inhomogeneity as well as susceptibility artifacts from bowel gas and metallic clips. The next technique described was a two-dimensional (2D) turbo spin-echo sequence. Takehara et al.⁶ applied this technique to 39 patients with chronic pancreatitis, demonstrating that dilatation and ductal narrow-

ing could be identified with quite high accuracy when compared with ERCP. This sequence, due to its spin echo nature, is less susceptible to local magnetic field inhomogeneity and motion as opposed to the previously used steady state free precession gradient echo sequence. However, it has the disadvantage of requiring a breath hold period of 45 to 60 s. This limits its use as debilitated or elderly patients with obstructive jaundice often cannot hold their breath for such a long period of time. The next technique described was a non-breath hold turbo spin echo MRCP technique by Outwater.⁷ These investigators used signal averaging to compensate for motion degradation that resulted from respiration. Although this technique accomplished a reduction, it, however, did not eliminate the effects of breathing on image quality.

In 1995, Barish et al.⁸ described a 3D non-breath hold T2-weighted Turbo spin-echo sequence with respiratory triggering where data acquisition was limited to the end expiration. At that point of the respiratory cycle, motion is minimal. Compared with the previous technique, this method provided improved resolution and increased signal-to-noise ratio. Furthermore, the non-breath hold nature of this technique permits its application to patients that cannot hold their breath for a long period of time. This technique has been applied to more than 200 patients with very promising results and merits a more detailed description. The examination was performed with commercially available software at 1.5 Tesla. The non-breath hold T2-weighted 3D turbo spin-echo respiratory triggered sequence is prescribed in the coronal plane from multislab acquisition modes, implementing 10, 1.8-cm-thick slabs with 40% overlap between adjacent slabs and 52-mm-thick partitions (TR/TE, 5000/240 ms, 1 signal average echo-train of 31, echo spacing of 15 mm per segment, field of view 240 mm, and matrix 186 × 256). A body coil is used and no oral or intravenous contrast is administered. Glucagon is not injected. Respiratory motion artifacts are decreased with respiratory triggering. The actual scan time varies between 11.5 to 16 min, depending on the patient's respiratory rate. After the raw data are acquired, projectional images are obtained with the use of a maximum intensity projection or surface-shaded display algorithm. From the set of source images, the volume to be used is chosen so that a targeted reconstruction to the biliary tree or pancreatic system is achieved. The resultant data are viewed from angles ranging between 15 and 30 degrees. With this technique, in 200 patients the normal common bile duct was visualized in 97% and the pancreatic duct in 80% of cases. Whenever there was biliary or pancreatic duct dilatation, this was correctly identified, and the site of obstruction was clearly demonstrated in 98% of common bile ducts and 92% of pancreatic ducts.¹

The most significant difference between gradient echo cholangiography and fast spin echo cholangiography is that the latter demonstrates higher signal-to-noise ratio and minimizes field inhomogeneity effects.⁹ These two differences result in an improved image quality.

Although there are no reports in the literature describing black bile MR cholangiography, Meakem and Schnall have reported a fast multiplanar spoiled

grass sequence where bile is dark.¹⁰ The sequence that these authors have used is a T1-weighted sequence resulting in images where the bile is black. Images are acquired in the coronal plane with a surface coil and a small field-of-view allowing high-resolution images to be obtained.

More recent techniques in MRCP include rapid imaging using fast spin-echo pulse sequences, as in half-fourier acquisition single-shot Turbo spin-echo (HASTE)¹¹ or steady state fast spin-echo (SSFSE)¹² performed in a single breath hold. These techniques have advantages over gradient recalled steady state free precession (SSFP) techniques. First, the inherent gain in signal/noise; second, less sensitivity to field inhomogeneities caused by varying susceptibility; third, it is the true T2-weighting as opposed to T2* weighting. The FSE techniques can be implemented in either a 2D or a 3D form. Miyakazi et al. used HASTE in a 2D form with either a sequential multislice or single slice acquisition.¹² The echo time of 87 ms provided T2 weighting. A single shot with half-Fourier acquisition of 240 lines and two acquisitions could be performed in 18 s for multislice and 2 to 3 s for a single slice and was accomplished in a single breath hold. The peritoneal fat was suppressed using fat saturation prior to data acquisition. The SSFP techniques have been available for several years, whereas the FSE techniques in a 2D or 3D form have become available only recently.

II. MRCP ADVANTAGES

Imaging the biliary tree with magnetic resonance imaging prompted investigators to use this modality because it is noninvasive, has inherent high-contrast resolution, without ionizing radiation; has multiplanar imaging capabilities; and, finally, the fact that it is not operator dependent, in contrast to ultrasonography, percutaneous transhepatic cholangiopancreatography, and endoscopic retrograde cholangiopancreatography. Furthermore, MRI offers the advantage of combining multiple tests, that is, in addition to the three-dimensional high-resolution images of the biliary tree and pancreatic ducts, multiplanar images of the upper abdomen can be obtained if one applies various sequences in one imaging session.¹⁰

III. PULSE SEQUENCES

At our institution, both breath hold and non-breath hold sequences (2D-FSE) have been used in the examination of the biliary system. MR examinations are performed on a Siemens Magnetom SP 4000 and the Siemens Magnetom Vision 1.5 Tesla (Siemens Medical Systems, Iselin, NJ). The basic fast spin echo sequence utilizes multiple 180° RF pulses to cover different phase-encoding steps in each TR cycle. Imaging is based on the echo-sharing scheme in which the total scan time is decreased by the number of echoes within a single TR loop. The echo spacing

and echo-train length were the only parameters varied in sequences to obtain the desired echo time. Two such pulse sequences were designed; the first sequence had an echo-train length (ETL) of 16 and a echo-spacing (ESP) of 11.375 ms and the echo was centered at 91 ms using the reordering scheme. The second pulse sequence had an ETL = 23, ESP = 22.5 ms and the center echo was centered at 270 ms. In addition, a phase cycling scheme was employed using preparatory RF pulses to avoid Eddy current-related errors in a final echo. Both pulse sequences were added with flow compensation along the read (frequency) direction. Due to the high ETL, the second sequence could be completed in 24 s and was performed easily in a breath hold mode. In this mode, four slices could be obtained in coronal or axial plane with a 10% gap using several breath holds and as a result, multiple slices were obtained covering the desired area of interest. In patients who were unable to hold their breath for 24 s, the same pulse sequence was used in non-breath hold mode with increased coverage and increased acquisitions. In addition, in three cases a turbo spin echo with half-fourier mode (HASTE) was used in a single shot to acquire 120 lines of data in 10 s. The resultant images from both modes were subjected to MIP algorithm. Individual partitions and the MIP images were simultaneously viewed. Conventional T1 and T2 spin echo and gradient echo pulse sequences were also used in our patients, depending on the underlying pathology. The protocol used at our institution is outlined in Table 1 and is summarized below:

1. Coronal non-breath-hold MRCP with turbo spin echo
2. Sagittal or coronal breath-hold MRCP with turbo spin echo
3. Sagittal or coronal breath-hold MRCP with HASTE
4. Axial T1-weighted spin echo with fat suppression
5. Axial breath hold T1-weighted FLASH (fast low-angle shot)
6. Axial breath hold FLASH post-contrast

IV. NORMAL MAGNETIC RESONANCE CHOLANGIOGRAPHY

In a patient with a normal nondilated biliary system, the structures that may be seen include the common bile duct (CBD), common hepatic duct, gallbladder, portions of the right and left hepatic ducts, and portions of the pancreatic ducts. These ducts are usually visible with a very obvious degree of resolution on MIP images obtained from a fast spin echo MR cholangiogram.^{7,13} Nondilated intrahepatic ducts are usually not seen on the MIP images. However, they are occasionally visible on the individual partitions. The dilated intrahepatic bile ducts can be visualized in almost 100% of patients.¹⁴ However, the nondilated intrahepatic bile ducts can be followed to the outer 1/3 of the liver parenchyma in more than 90% of patients.¹⁵ Regarding the main pancreatic ducts in the body and tail, it can be visualized in 96% of cases.¹⁶ The ventral pancreatic duct at the pancreatic head site has been visualized in 95% of cases, whereas the dorsal pancreatic duct remnant

TABLE 1
Imaging Parameters Used in MRCP

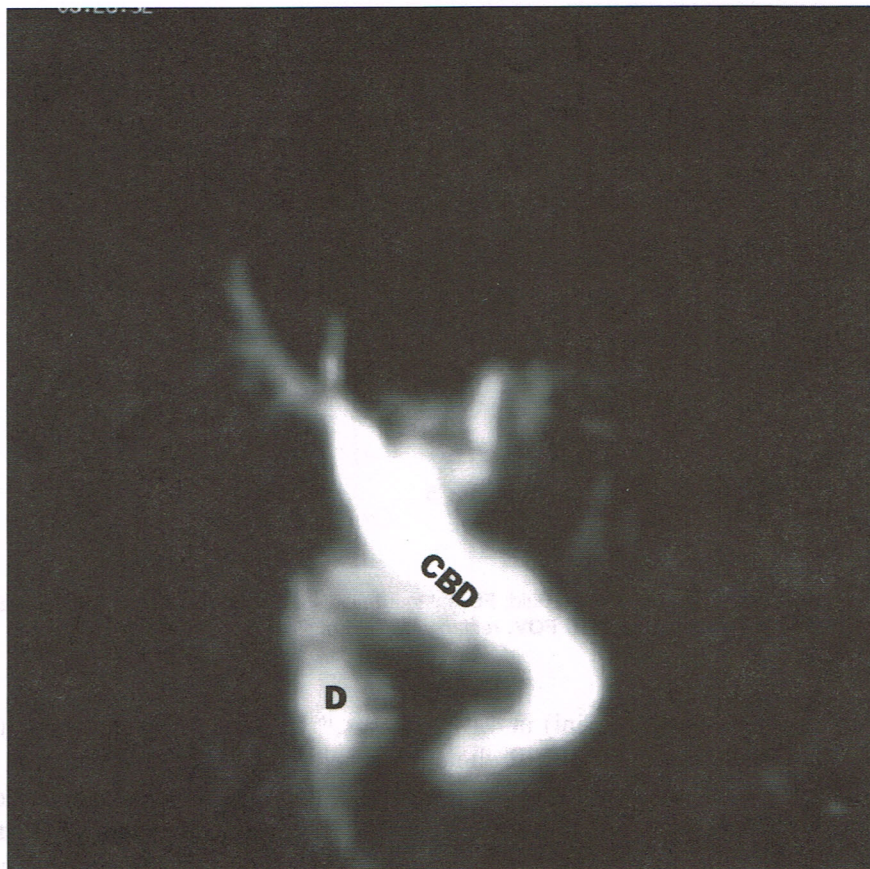
Sequence	TR (ms)	TE (ms)	SL (mm)	Matrix	FOV (mm)	ACQ
TSE coronal/ sagittal	7000–10,000	91 or 270	4 (10% gap)	138 × 256	340–420	2–6
HASTE Coronal/ sagittal	10.92	87 flip = 150	5	240 × 256 half-fourier	300–380	1
T1-FS axial	650	15	2	192 × 256 3/4 REC FOV	330–400	1
T1-GRE axial	140	6 flip = 80	5	144 × 256 3/4 REC FOV	330–400	1

Note: **TSE:** turbo spin echo; **BH:** breath hold; **FS:** fat saturation; **GRE:** gradient echo; **HASTE:** half-fourier single shot turbo spin echo; **REC FOV:** rectangular field of view.

is visualized (duct of Santorini) in 42% of cases.¹⁶ In a recent report by Reuther et al.,¹⁷ they used a single-shot MR cholangiography technique and compared the result with intravenous cholangiography (IVC) for visualization of gallbladder, bile ducts, cystic duct, and intrahepatic ducts. The gallbladder was adequately visualized with IVC in 77% of patients and with MRC in 88%. Rates for visualization of the CBD were 97 and 100%, for cystic duct 27 and 75%, and for intrahepatic ducts 28 and 77%. With either technique, calculi in the gallbladder were correctly predicted as solitary or multiple in nearly 80% of patients.

V. PATHOLOGIC CONDITIONS

A variety of pathologic conditions of the hepatobiliary and pancreatic system can be evaluated by MRCP. These may cause biliary and/or pancreatic ductal dilatation, irregularity and deformity of the biliary system, or the lesions may be due to a congenital abnormality. As a result, the disease entities that may be evaluated by MRCP include post-cholecystomy changes (Figures 1 and 2), choledocholithiasis (Figure 3), cholangiocarcinoma (Figure 4), pancreatic carcinoma (Figure 5), pancreatitis, ampullary carcinoma, obstructing lymph nodes (Figure 6), congenital anomalies of the biliary tree, congenital anomalies of the pancreatic ducts and pancreas, inflammatory conditions, Caroli's disease (Figure 7), pancreatic duct calculi, pseudocysts, pancreas divisum, and ductal dilatation. We do illustrate most of these conditions.



A

FIGURE 1 (A–C). After cholecystectomy. This 81-year-old female referred for exclusion of a distal common bile duct obstruction. She had remote history of cholecystectomy. (A) MIP of coronal non-breath hold FSE T2 images reveals a common bile duct (CBD), which is 1.8 cm dilated. Duodenum: D. (B) MIP of coronal breath hold FSE T2 images reveals dilatation of the common bile duct (CBD) and intrahepatic ducts. Notice that the distal aspect of the common bile duct (arrow) is not identified, probably due to spasm of the sphincter of Oddi given the normal ERCP images shown below. (C) ERCP shows dilatation of the intra- and extrahepatic biliary tree without evidence of an obstructing lesion (as was also proven by CT).

A. Diseases Causing Bile Duct Obstruction

The sensitivity of MRCP for bile duct obstruction ranges from 91 to 100%, and the site of obstruction (Figures 5 and 6) can be detected in 85 to 100% of cases.¹⁴ However, the cause of obstruction, as well as differentiation between high-grade



FIGURE 1B

stenosis and complete obstruction cannot be regularly demonstrated.² Because MRCP is a modality that demonstrates the bright bile that exists within the ducts at the time of imaging, duct caliber measurements are not necessarily in agreement with those determined by ERCP. That is because during ERCP the ducts may be over or under filled with contrast. Occasionally, under filling may be intentional and done to avoid inducing septicemia. If there is distension of the ducts during ERCP, this may occur between the site of injection and an area of obstruction along the biliary tree. In a recent report by Lee et al.,¹⁸ the results of 3D MRCP was compared with those of ERCP. The authors were able to determine the level of obstruction in 91% with MRCP and in 83% with ERCP. Their sensitivity, specificity, and accuracy in distinguishing malignant from benign lesions were 81, 92, and 87%, respectively, for MRCP and 71, 92, and 83%, respectively, for ERCP. In their opinion, these two modalities have equivalent diagnostic value.

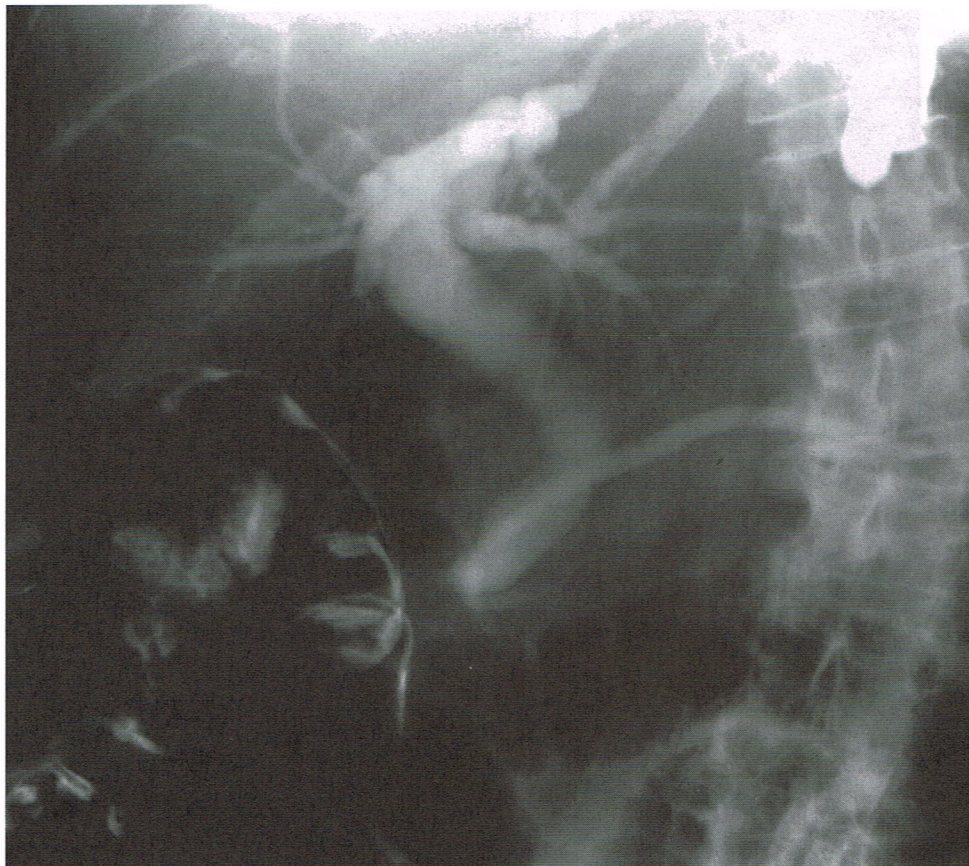
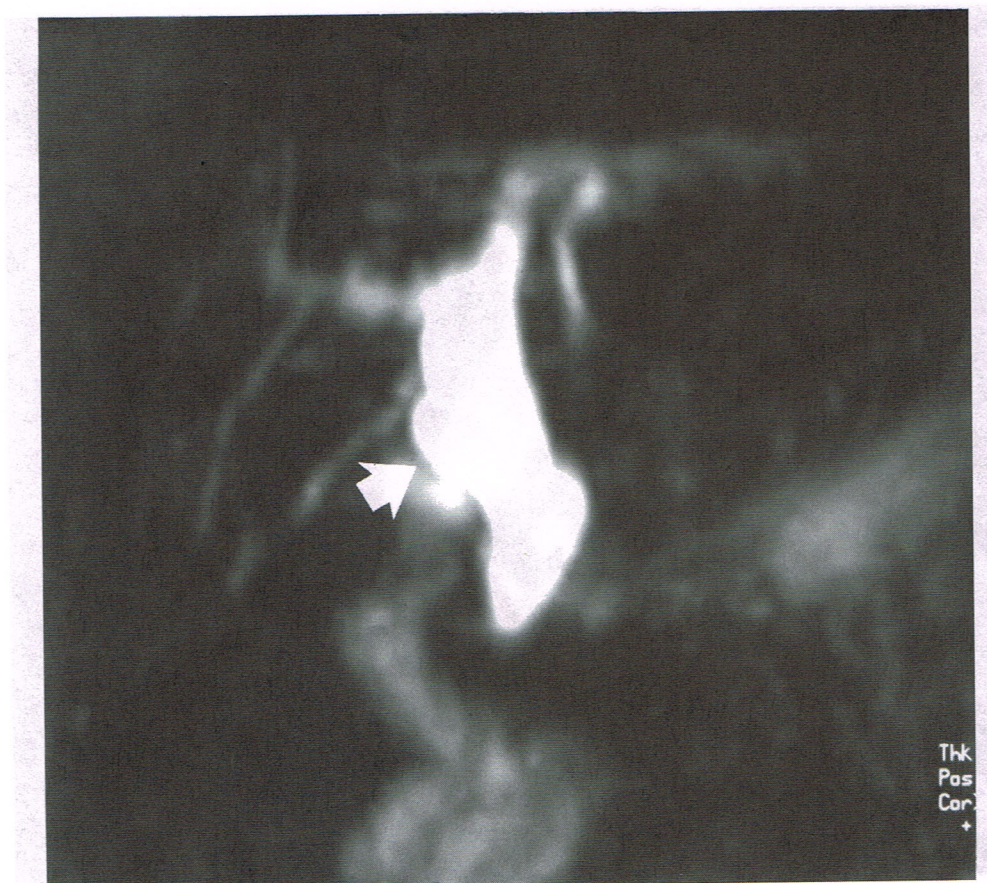


FIGURE 1C

The pathologic entities that can cause biliary duct dilatation from obstruction include choledocholithiasis, cholangiocarcinoma, pancreatic carcinoma, ampullary carcinoma, inflammatory causes, injuries to the biliary ducts, and sclerosing cholangitis. Conditions such as Caroli's disease and choledochocoele are discussed in the section on Biliary Cystic Disease.

B. Choledocholithiasis

The noninvasive diagnosis of CBD stones remains a challenge for the radiologist. The sensitivity of ultrasonography in the diagnosis of choledocholithiasis ranges from 20 to 80%.^{19,20} The sensitivity of CT ranges from 23 to 85%.^{19,21} Whenever a stone is seen in sonography or CT, the diagnosis can often be



22 A 100%

FIGURE 2 (A-C). Choledochal cyst. Type 1 choledochal cyst in a 69-year-old female with a remote history of cholecystectomy who presented with elevated alkaline phosphatase and recurring abdominal pain. (A) MIP of coronal non-breath hold FSE T2 images reveals fusiform dilatation of the common bile duct consistent with a Type 1 choledochal cyst. However, its margins, as well as the intrahepatic duct margins, are blurred due to motion artifacts despite averaging of motion artifacts with eight acquisitions. Arrow shows-cystic duct remnant. (B) MIP of coronal breath hold FSE T2 images (with caudal angulation) illustrates the choledochal cyst with sharp margins. Fluid in the duodenal bulb (b), stomach (s), and large bowel (B) is also noted. The distal aspect of the cystic duct remnant (arrow) is identified with a low insertion. The normal pancreatic duct (small arrows) is also identified. (C) ERCP confirms the Type 1 choledochal cyst and a low insertion of the cystic duct remnant (arrow).

established. However, when the stone is not seen, direct opacification of the bile ducts is frequently necessary for proper diagnosis. In this regard, ERCP is often deemed to be the examination of choice, as diagnosis and treatment may be

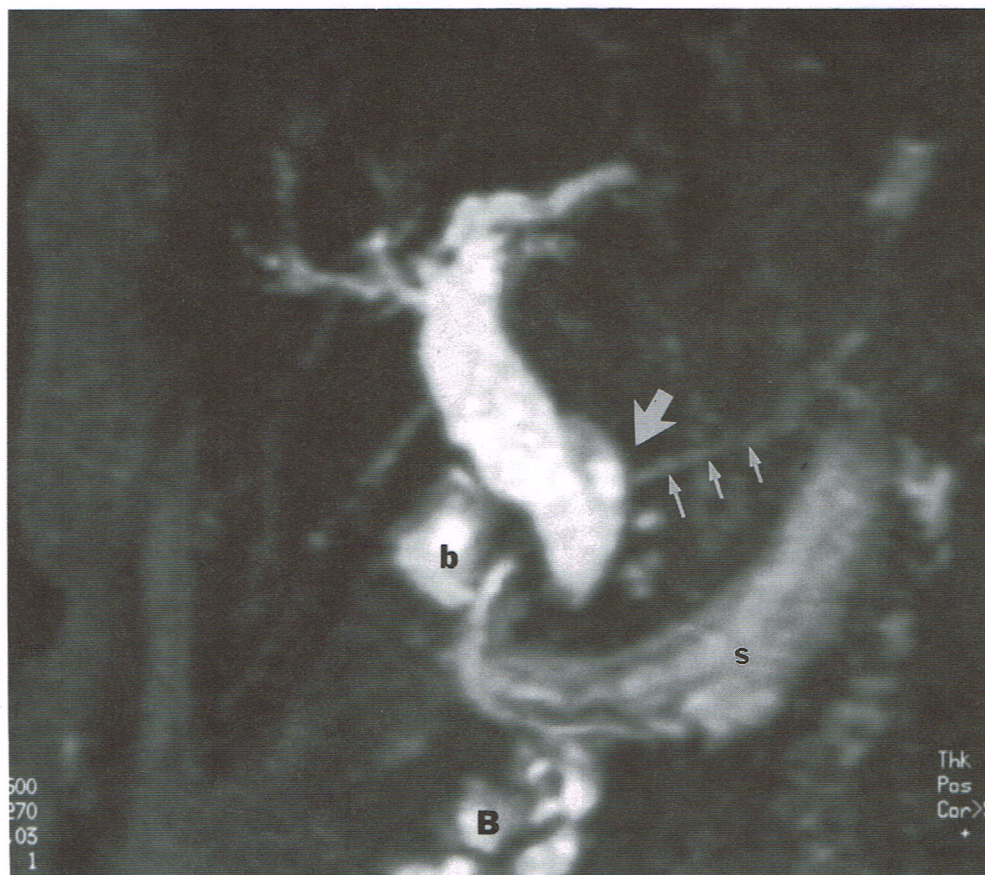


FIGURE 2B

undertaken at the same time. However, ERCP is an invasive modality for diagnosing a simple condition such as choledocholithiasis.

The detection of choledocholithiasis is one of the common aims of MRCP (Figure 3). Guibaud et al. evaluated the use of MR cholangiography in the diagnosis of choledocholithiasis.²² They used the two-dimensional T2-weighted turbo spin echo sequence and were able to detect stones as small as 4 mm in their series of the 10 patients they examined. The signals of the stones in their study were very low, and they were all homogeneously dark with no rim or laminated appearance. Their patients had a total of eight stones and these were visible in 8 of 10 coronal images, 6 of 10 axial images, and 4 of 10 oblique images. In the 3D MIP reconstructions, the stones were seen in five of the coronal sets and six of the axial sets. They obtained the best results with use of the multiplanar reconstruction software, where 9 of the 10 coronal sets and 8 of the 10 axial sets showed stones

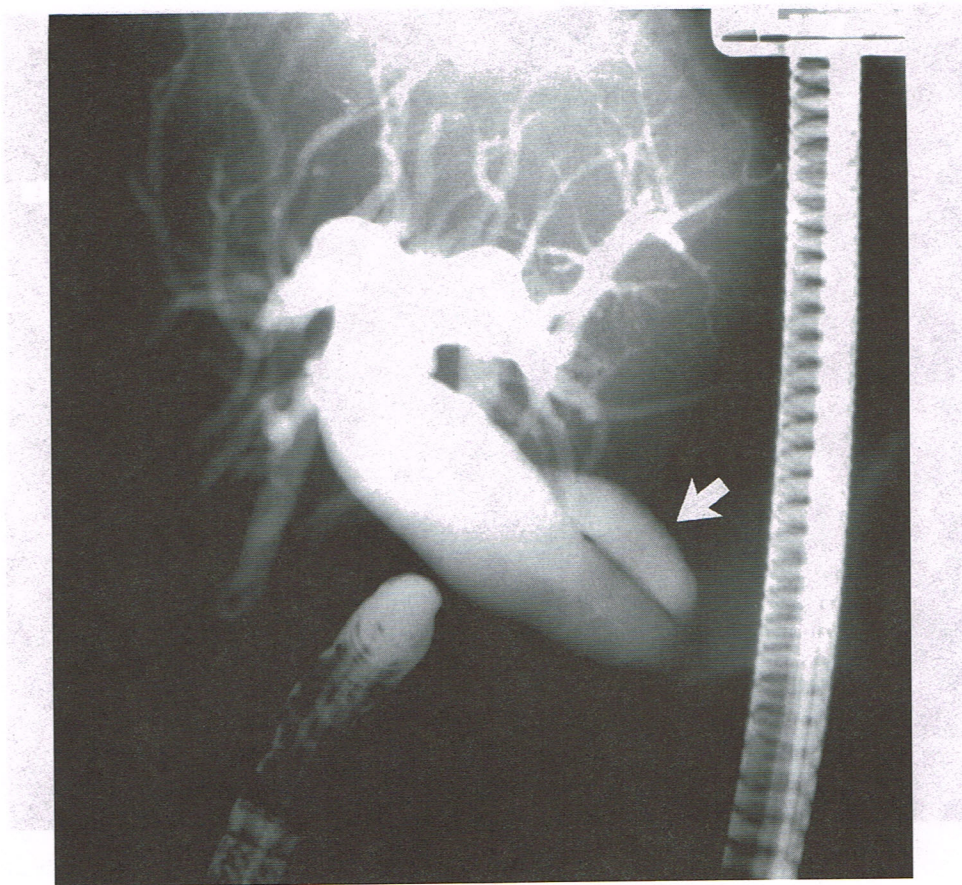
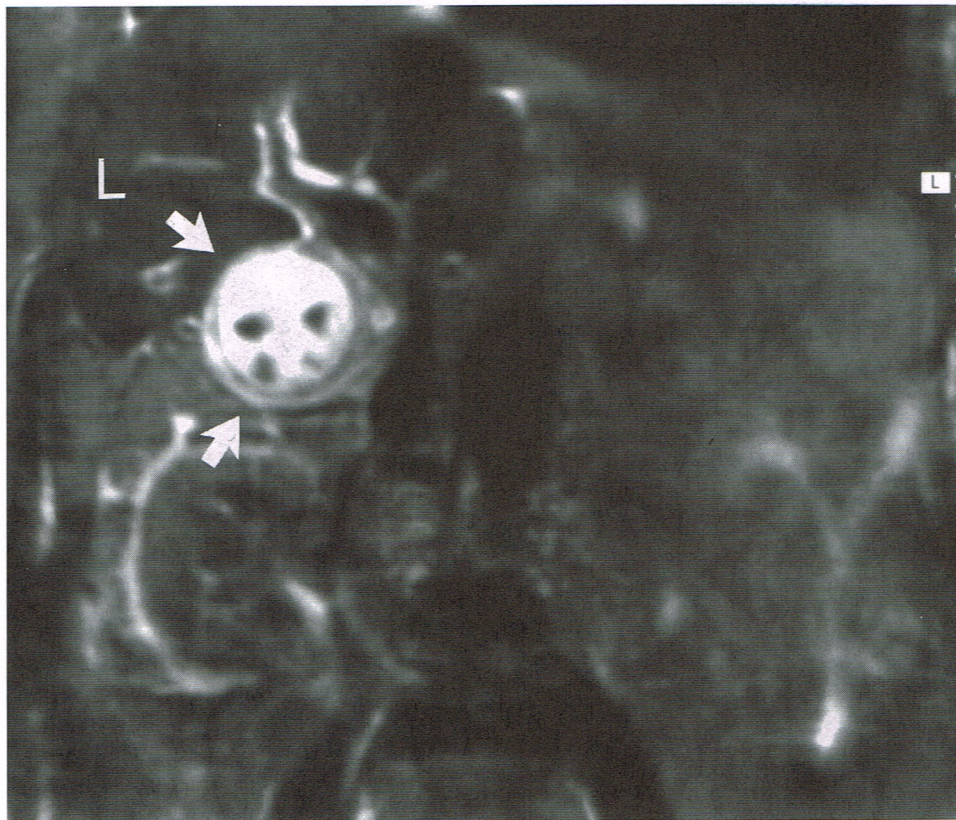


FIGURE 2C

in the bile ducts. The combination of the 3D MIP and the multiplanar reconstructed images enabled detection of choledocholithiasis in all 10 patients. The same investigators²² detected stones in 26 of 32 patients with proven choledocholithiasis. The sensitivity was 80% and the specificity 98%. Again, the smallest stone detected in the CBD was 4 mm. Unusual causes of intraductal filling defects such as blood clot, tumors, and migrating parasites can also be displayed and must be differentiated from calculi. Sludge or various small stones impacted in the ampulla are, however, difficult to distinguish from ampullary stenosis or neoplasm. Overall, the reported sensitivities in the diagnosis of choledocholithiasis have varied from 71%¹⁵ to 100%.^{22,23} Those investigators used a 2D fast spin echo technique. Soto et al,²³ using a 3D fast spin echo respiratory triggered sequence, reported a sensitivity of 100% and stressed the importance of a careful study of the source images prior to examining the MIP results.



A

FIGURE 3 (A-G). Cholecystitis, cholangitis, and choledocholithiasis. **Case 1.** Ascending cholangitis and cholecystitis due to choledocholithiasis in an 80-year-old man with right upper quadrant pain, jaundice, and fever. (A) Coronal non-breath hold FSE T2 image shows gallbladder with a thickened wall due to cholecystitis with gallstones (arrows). Liver (L). (B) MIP of coronal non-breath hold FSE T2-weighted images shows the impacted CBD stone distally (arrow). The gallstones and additional CBD stones that were demonstrated on the individual slices, however, are not identified on the projected image due to their obscuration from overlying fluid. This is a potential pitfall and stresses the need for evaluation of individual images in addition to MIP. **Case 2.** This 63-year-old woman presented with nausea and vomiting. (C) MIP of the coronal non-breath hold FSE T2 images shows dilatation of the intra- and extrahepatic biliary system. No filling defect is seen in CBD. (D) MIP of the coronal breath hold FSE T2 images shows dilated biliary system and a rounded filling defect in the distal CBD (curved arrow). At surgery, an impacted distal CBD stone was confirmed and no neoplastic process was found.

C. Cholangiocarcinoma

The role of imaging in such patients is establishment of the diagnosis, tumor extent, and to determine the approach for palliative drainage if the tumor is

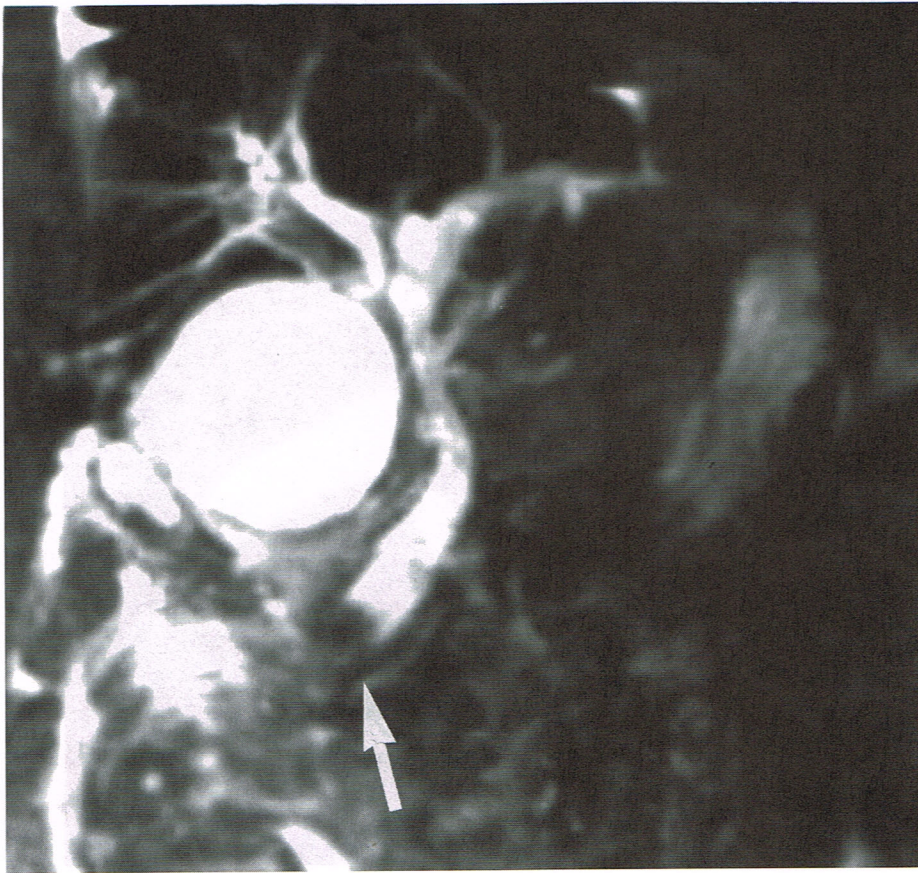


FIGURE 3B

unresectable. Assessment of the extent of the tumor requires direct opacification of the ducts proximal and distal to the tumor. However, in cases where the tumor extends beyond the porta hepatis, ERCP will usually demonstrate the ducts distal to the obstruction, whereas transhepatic cholangiography will usually demonstrate the ducts proximal to the tumor. The advantage of MRCP in such cases would be the demonstration of the ductal system above and below the stenosis. Coronal 3D MIP reconstructions facilitate demonstration of the biliary tree above and below the stenosis, and coupling those images with axial, targeted MIPs that encompass the bile duct bifurcation, the evaluation of tumor extent is more complete.^{11,14}

D. Pancreatic Carcinoma

The diagnostic value of MRCP in such patients is limited as most pancreatic carcinomas are unresectable at the time of presentation and the diagnosis is

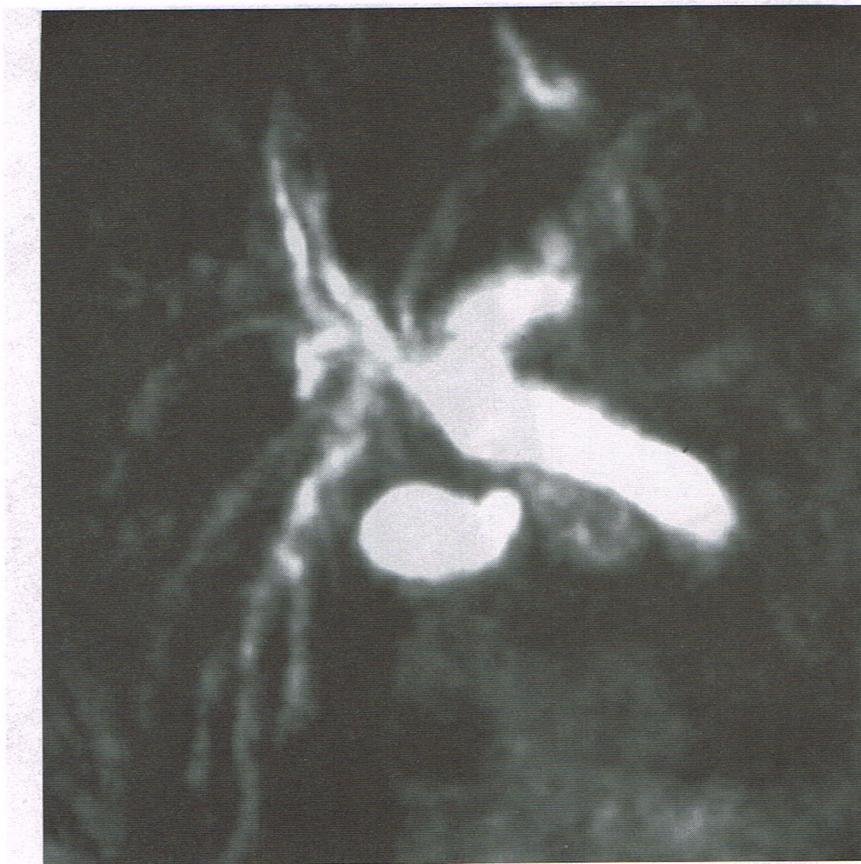


FIGURE 3C

established with CT or ultrasonography. However, information regarding the pancreatic and biliary duct proximal to the stenosis or obstruction can be obtained that may facilitate endoscopic stenting if this procedure is under consideration.¹⁴

E. Ampullary Carcinoma

In this type of malignancy, ERCP offers the advantage of direct visualization of the ampulla and biopsy performance at the same time. In a recent study, only 2/6 ampullary carcinomas were correctly diagnosed by MRCP,²⁴ although the site of obstruction was correctly assessed.

F. Inflammatory Stenosis and Bile Duct Injuries

Patients with CBD dilatation after cholecystectomy, odditis, and those with a dilated CBD after having passed a stone are better evaluated with ERCP in

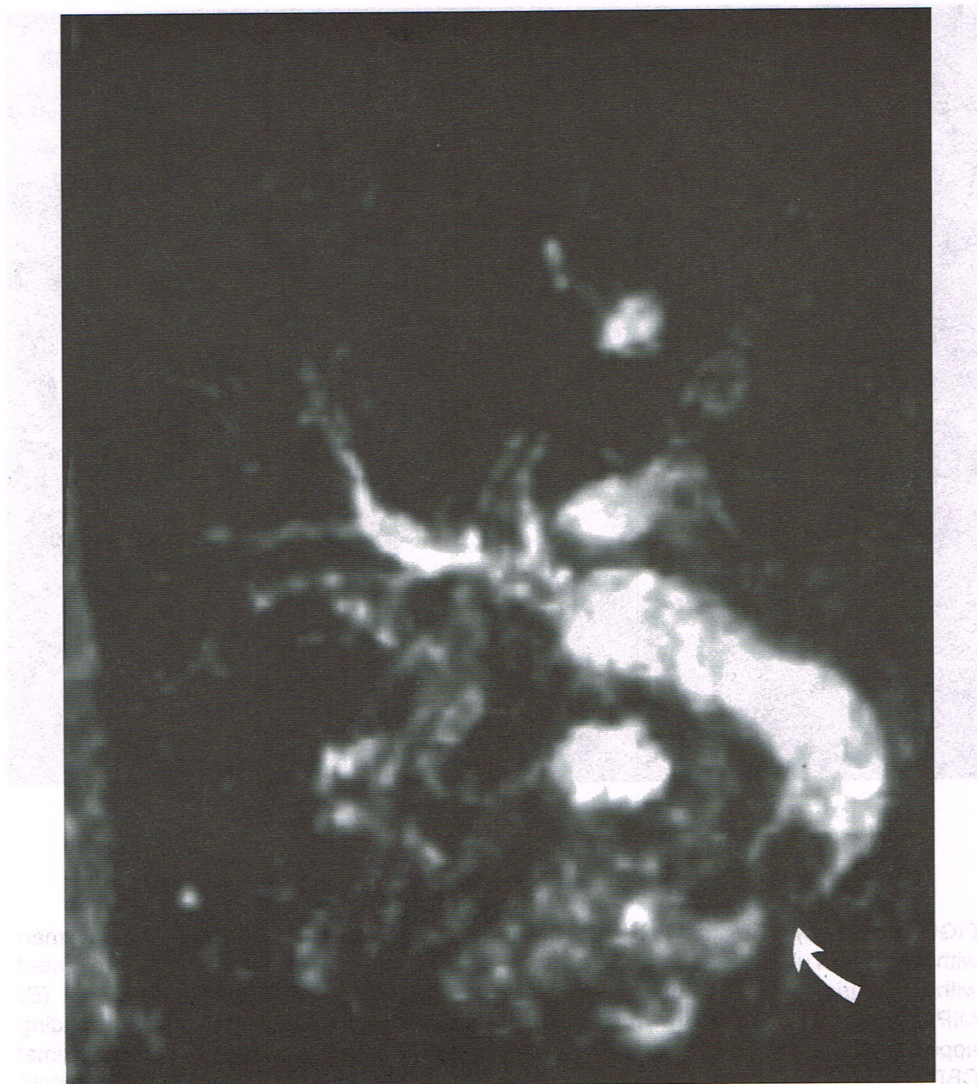
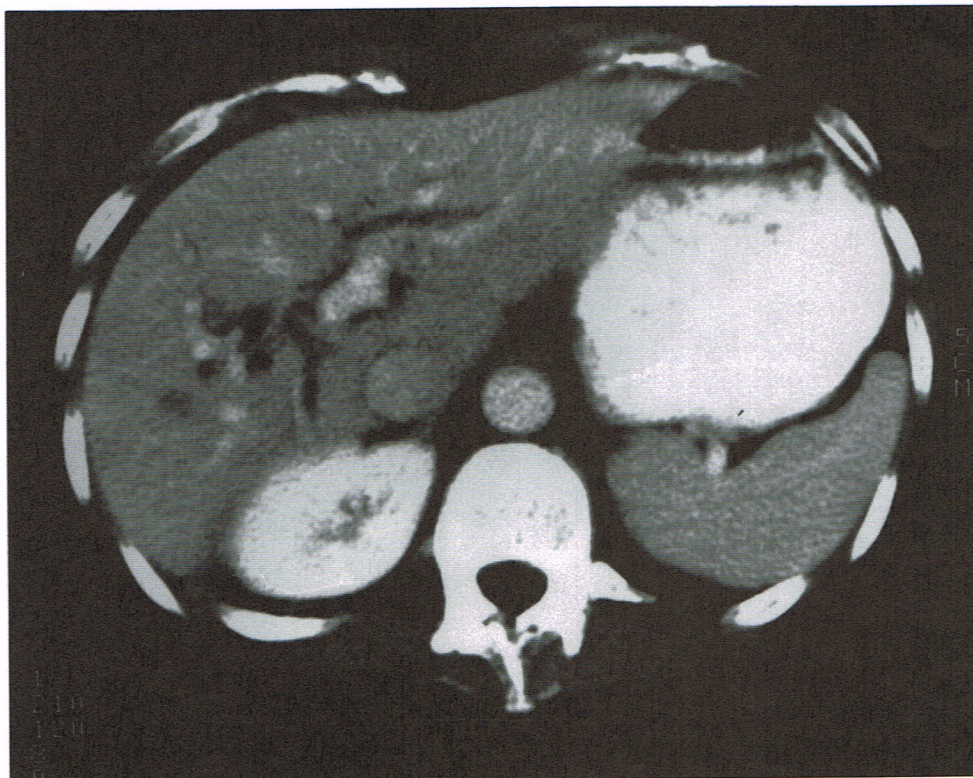


FIGURE 3D

conjunction with their symptomology and other laboratory data. MRCP may only provide information regarding duct diameter. Furthermore, MRCP is inferior to ERCP in terms of evaluating the ampullary area.^{14,25}

G. Pancreatitis

CT and ultrasound are the imaging modalities of choice for diagnosing acute pancreatitis. Performing a diagnostic ERCP in the acute setting in order to diagnose



A

FIGURE 4 (A–C). Sclerosing cholangitis and cholangiocarcinoma. A 45-year-old woman with a history of ulcerative colitis who had undergone a total colectomy in the past presented with epigastric pain. (A) Abdominal CT showing mildly dilated intrahepatic bile ducts. (B) MIP of the coronal breath hold FSE T2 images demonstrates dilatation and a beading appearance of intrahepatic ducts. The distal common hepatic duct as well as the proximal CBD could not be seen. Paucity of bile (arrow) is observed at the area of the junction of right and left hepatic ducts. (C) ERCP at the right posterior oblique position shows an area of marked stenosis involving the common hepatic ducts. Brushings from the stenotic area were suggestive for the diagnosis of sclerosing cholangitis. However, as a definitive diagnosis could not be established, laparotomy was undertaken that revealed the presence of cholangiocarcinoma in the stenotic area involving the distal left and right hepatic ducts (Klatskin's tumor).

gallstone pancreatitis remains controversial, as complications with ERCP occur more frequently.²⁶ MRCP may have a role in diagnosing choledocholithiasis in such patients; nevertheless, its accuracy has not yet been determined.¹⁴ In cases of chronic pancreatitis where ductal narrowing is a common feature of the disease, MRCP results agree with ERCP findings in 70 to 92% of cases of ductal narrow-

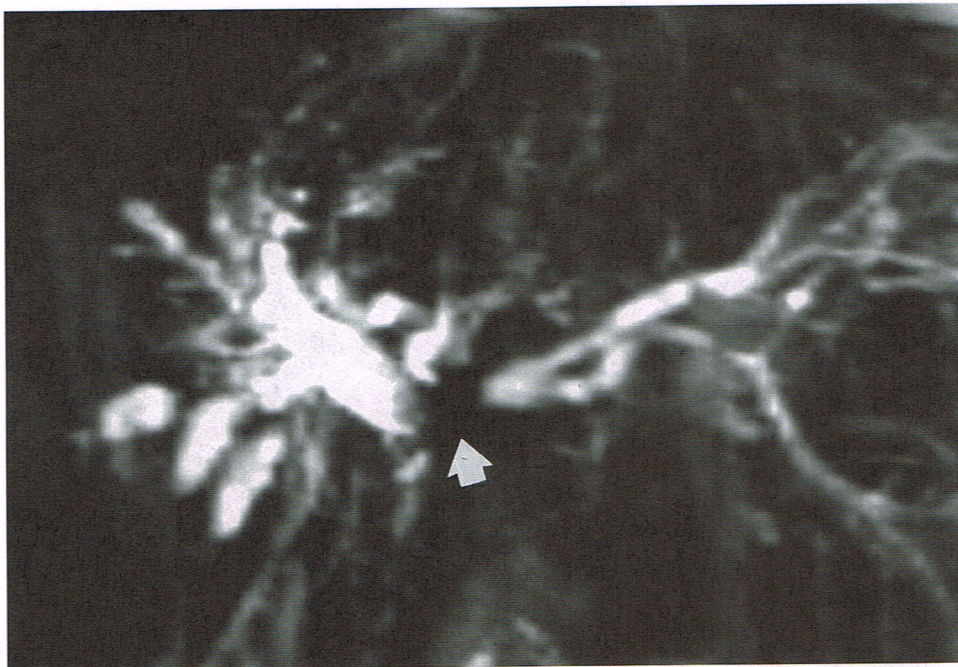


FIGURE 4B

ing.⁶ It should be noted that technical factors did not enable those investigators to demonstrate side branch narrowing reliably. However, their technique enabled them to detect intraductal calculi.

H. Sclerosing Cholangitis

This is an idiopathic disorder consisting of a diffuse periductal inflammatory process that may progress to biliary cirrhosis. Approximately 70% of these patients have inflammatory bowel disease, most commonly ulcerative colitis. Once large ducts are involved, the study of choice for establishing the diagnosis is cholangiography. Findings include diffuse multiple focal areas of strictures involving both intrahepatic and extrahepatic bile ducts (Figure 4). Most commonly, intrahepatic duct abnormalities are present and it is uncommon for isolated extrahepatic disease to be present. The dilated duct segments result in a beaded duct appearance from alternating normal duct segments and strictures. Other typical cholangiographic features include mural irregularities, diverticulum-like outpouches, and lack of arborization of intrahepatic biliary radicles (duct pruning). Due to the sclerosing nature of this disease, the ductal dilatation proximal to strictured regions is mild or

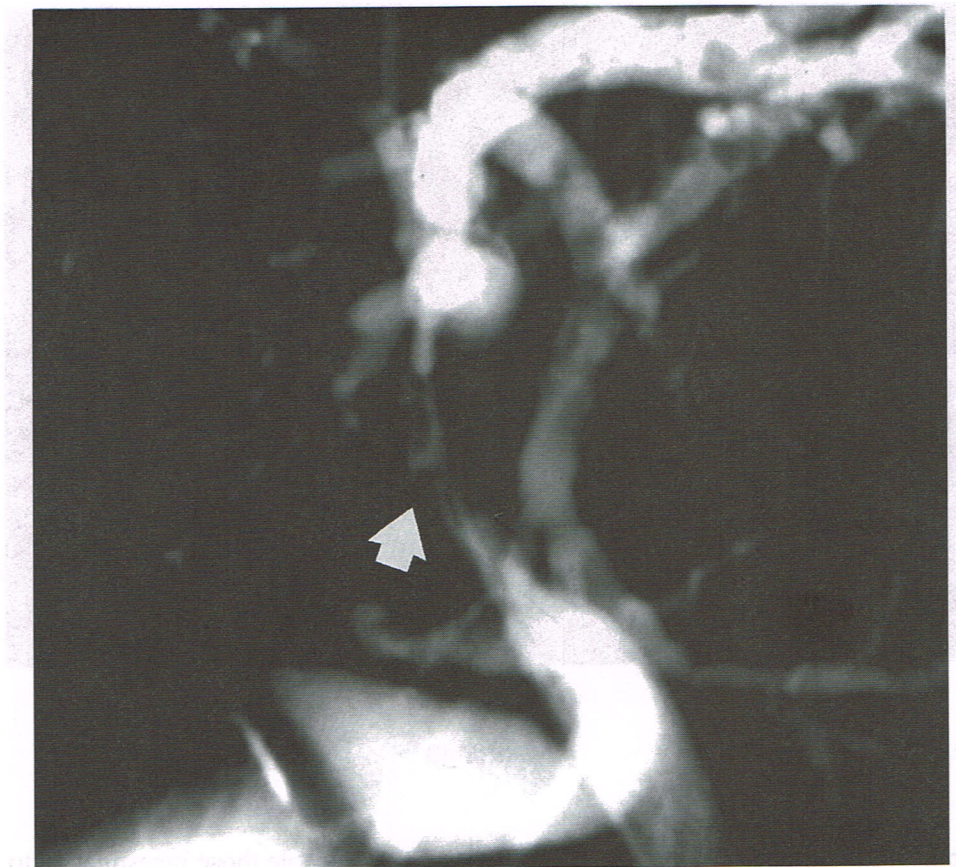
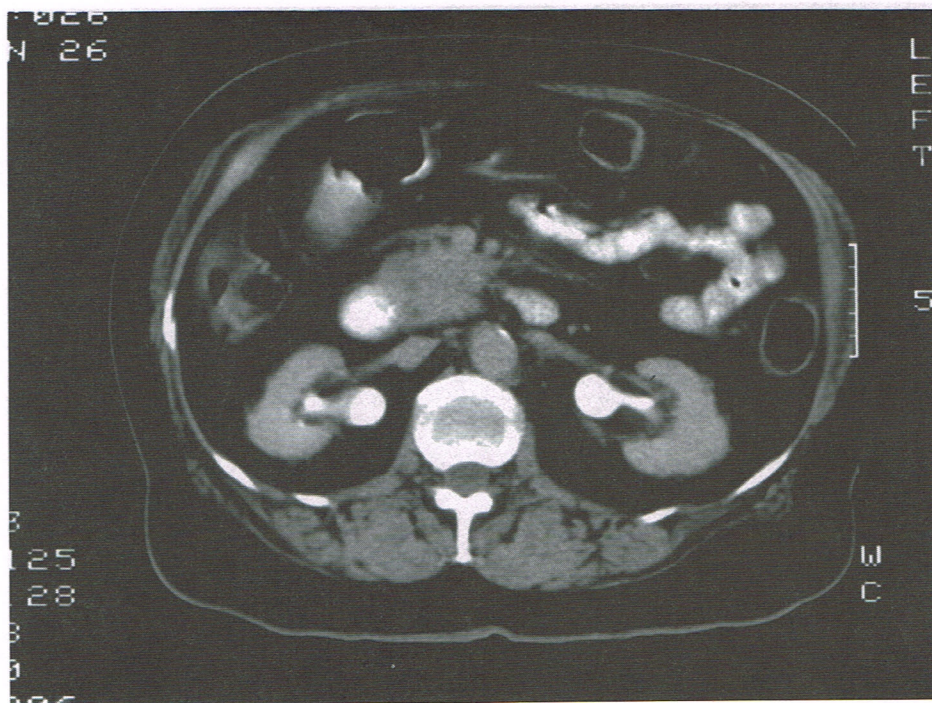


FIGURE 4C

moderate. Once marked dilatation is present, this raises the suspicion of a superimposed cholangiocarcinoma. Nevertheless, a dominant severe stricture may also result in marked ductal dilatation. CT and ultrasonography cannot demonstrate the disease in detail as cholangiography does. However, it can be suggested by intrahepatic ductal dilatation in a scattered nonconfluent pattern (skip-dilatations), which is highly suggestive of the disease, as obstruction from other conditions causes confluent dilatations.

I. Biliary Cystic Disease

Congenital bile duct cysts present as dilated segments of the biliary ducts that are in communication with the biliary system. These may be single or multiple and may involve intra- or extrahepatic ducts or both. A comprehensive classification



A

FIGURE 5 (A-E). Pancreatic carcinoma. **Case 1.** A 74-year-old female presented with right upper quadrant pain and jaundice. ERCP was unsuccessful. (A) Contrast-enhanced CT shows fullness of the pancreatic head. (B) Axial T1-weighted fat saturation image shows a diffuse low signal of the pancreatic head (arrows) compared with that of the liver. Findings suggested chronic pancreatitis or tumor. (C) Axial contrast-enhanced gradient echo (FLASH) image shows an ill-defined area of low signal within the pancreatic head (arrow) due to either chronic focal pancreatitis or pancreatic carcinoma. (D) MIP of coronal non-breath hold FSE T2 images shows dilatation of CBD (19 mm), intra-and extrahepatic biliary tree as well as the pancreatic duct (5 mm) (small open arrows). Irregular narrowing of the distal CBD (large open arrow) is noted. Because neoplasm was of primary concern, the patient was operated on and the diagnosis of pancreatic head carcinoma was confirmed. **Case 2.** A 55-year-old woman presented with epigastric pain. (E) Coronal HASTE image reveals a markedly distended common bile duct (cbd) terminating abruptly at the pancreatic head. CT scan (not shown) disclosed a pancreatic head tumor that was proven by fine needle aspiration to represent adenocarcinoma.

has been developed by Todani in 1977 and is based on location, number, and shape of cyst or dilatation.²⁷ More analytically, this classification is highlighted as follows: Type 1A, saccular cystic dilatation of the common bile duct; Type 1B, focal dilatation of the common bile duct; Type 1C, fusiform dilatation of the common duct; Type 2, choledochal diverticulum; Type 3, choledochocoele; Type

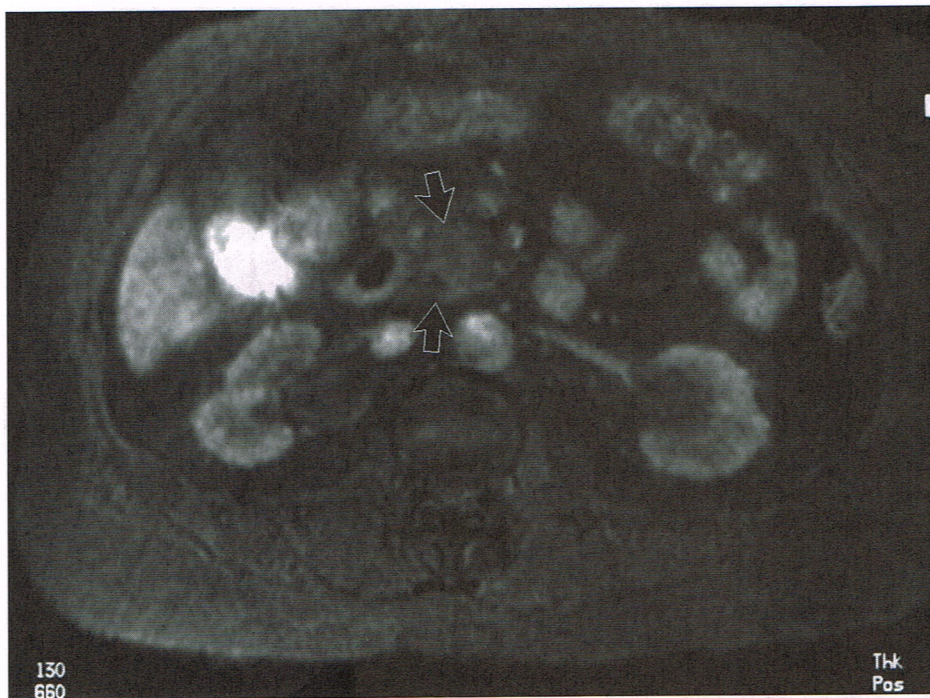


FIGURE 5B

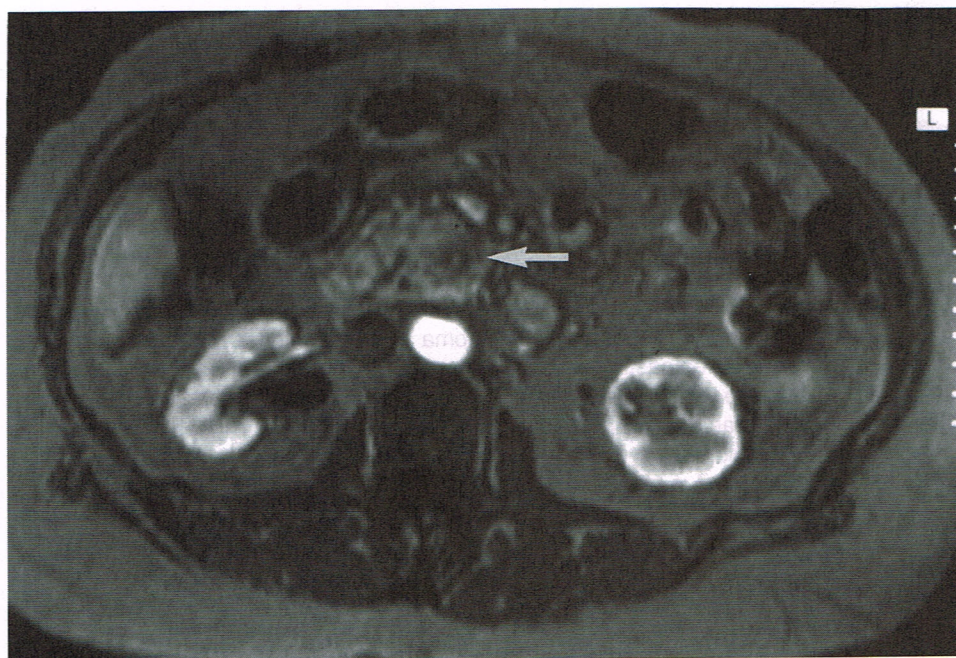


FIGURE 5C

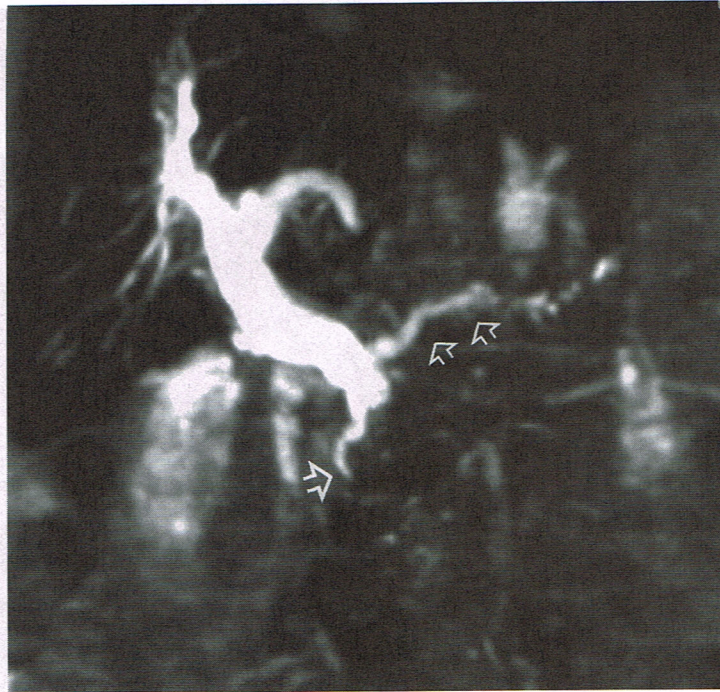


FIGURE 5D

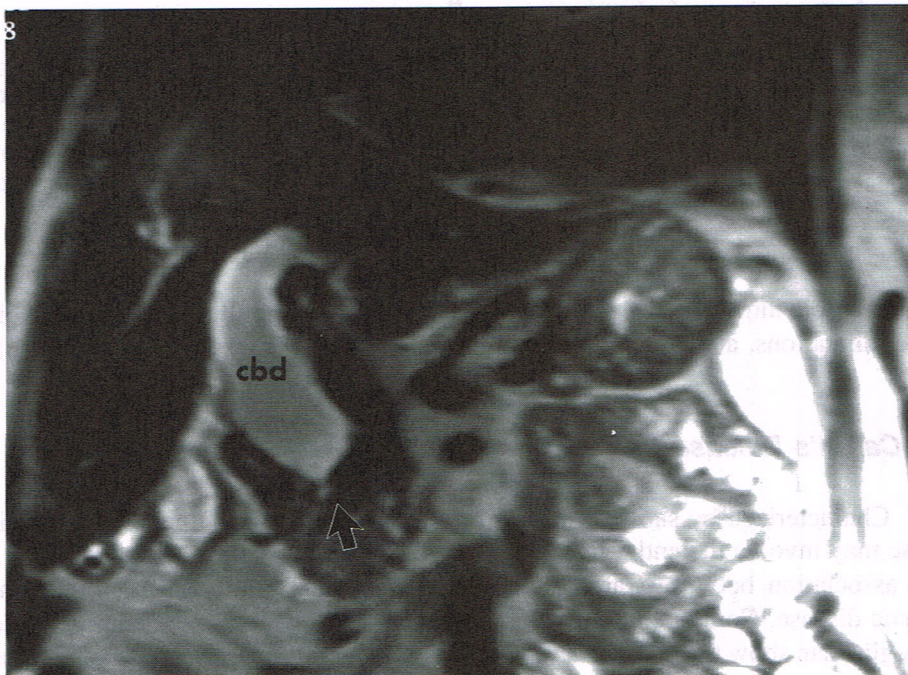
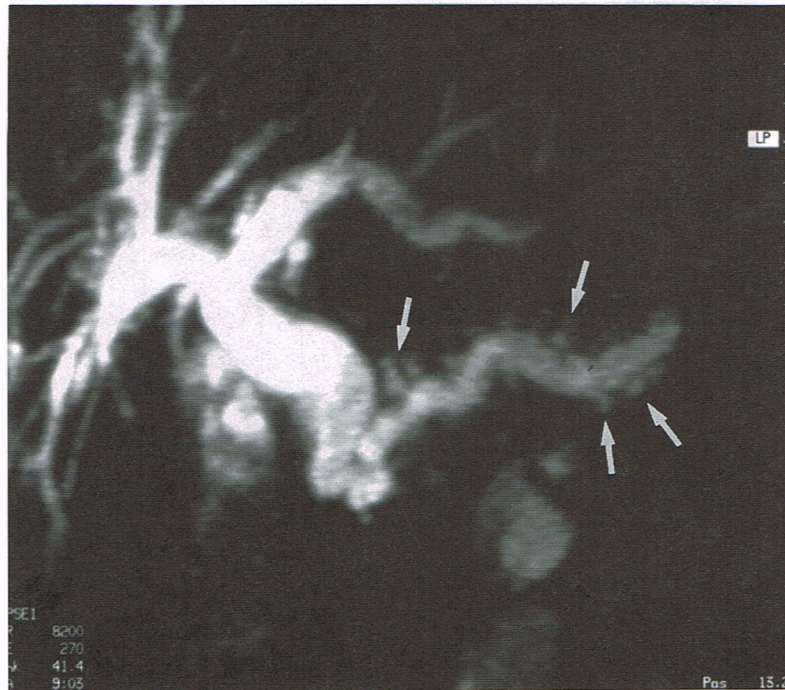


FIGURE 5E



A

FIGURE 6 (A–B). Nodal obstruction. A 63-year-old woman with history of colon carcinoma presented with gradual onset of painless jaundice. (A) MIP of the coronal non-breath hold FSE T2 images demonstrating dilatation of both the biliary and pancreatic ducts. Note is made of the intraparenchymal pancreatic ductal dilatation (small arrows), suggesting chronic obstruction. (B) PTC demonstrates abrupt termination of the CBD due to hilar nodal metastatic disease proven by CT for which the patient received radiation.

4A, multiple intra- and extrahepatic bile ducts; Type 4B, multiple extrahepatic bile duct dilatations, and Type 5, multiple intrahepatic duct cysts (Caroli's disease).

1. *Caroli's Disease*

Characterized by saccular ectasia of the intrahepatic bile ducts, Caroli's disease may involve the entire liver or can be confined to a single segment. There is an association between Caroli's disease, congenital hepatic fibrosis, and renal cystic disease. Computed tomography, ultrasonography, and magnetic resonance imaging can show the bile duct cysts as fluid-containing structures. Although those features are highly suggestive, direct cholangiography nevertheless is necessary to prove that those cysts are in direct communication with the biliary system and also

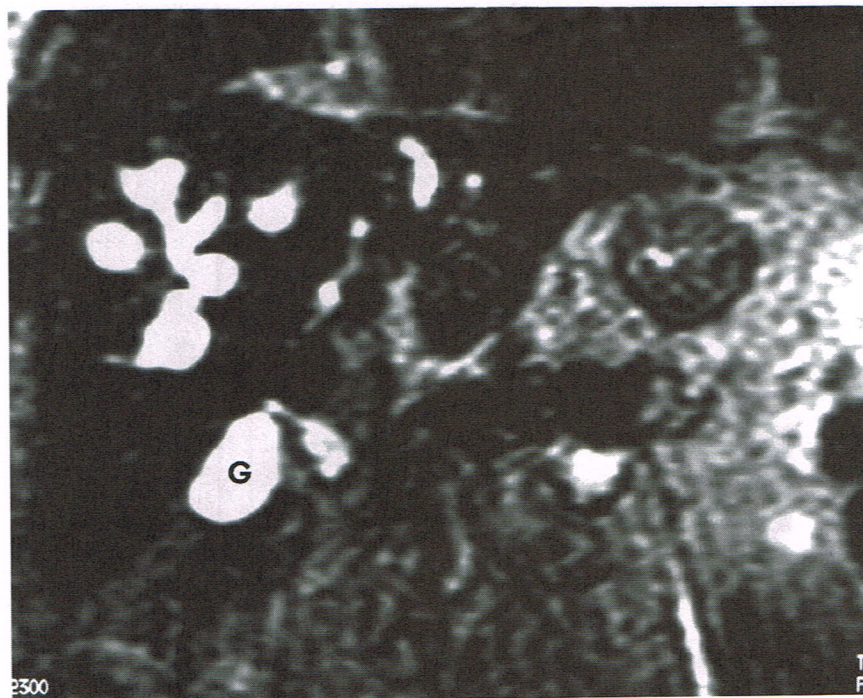


FIGURE 6B

to more accurately define the type of cystic disease. MR cholangiography can demonstrate those cystic dilatations because they are filled with bile. In the case we illustrate in Figure 7, the appearance of the biliary tree is suggestive of this disease entity; however, the relationship of the saccular structures to the biliary tree is not well appreciated due to the overlapping nature of the MIP image. Study of the individual partitions further demonstrates the relationship of the saccular outpouchings to the biliary tree.

III. ANATOMIC VARIANCE

MRCP has shown to be an accurate examination in the detection of normal anatomic variance of the bile ducts.²⁵ The identification of those variants for surgical dissection, according to some authors, would result in a decreased rate of bile duct injury and justifies the routine use on intraoperative cholangiography. The latter, however, remains controversial. Although MRCP can detect normal anatomic variance of the bile ducts, its routine use cannot be advocated before every laparoscopic cholecystectomy. However, it may prove useful in such patients presenting with additional factors for bile duct pathology, such as obesity, cholecystitis, prior abdominal surgery, or increased fat in the porta hepatis.



A

FIGURE 7 (A–C). Caroli's disease. This 40-year-old man was diagnosed recently to have Caroli's disease. (A) Coronal breath hold FSE T2 image reveals multiple communicating intrahepatic cystic structures. Their relationship to the intrahepatic ducts were better appreciated on the individual images. G: Gallbladder. (B) MIP of coronal breath hold FSE T2 images once again reveals multiple saccular communicating intrahepatic dilations. However, their relationship to the biliary tree is not well appreciated due to their overlapping nature. This case again illustrates the importance of evaluating the individual slices along with the MIP images. The non-breath hold MRC in this patient was suboptimal due to motion artifacts acquired over the 8 min of imaging time. CBD: common bile duct. G: gallbladder. (C) Corresponding ERCP confirms the MRC diagnosis of Caroli's disease.

A. Pancreas Divisum

Pancreas divisum is not an uncommon anatomic pancreatic variance. The clinical significance of pancreas divisum is that it has been held responsible for recurrent episodes of pancreatitis, and the diagnosis is made confidently with ERCP. However, in a series of 108 MRCP cholangiograms correlated with ERCP, six cases of pancreas divisum were shown, both by MRCP and ERCP, yielding a sensitivity, specificity, negative, and positive predictive values of 100%.¹⁶

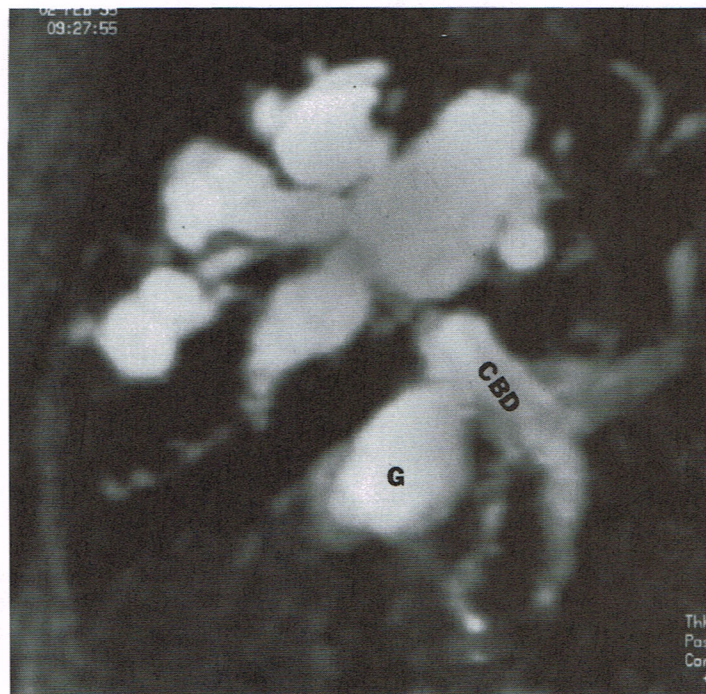


FIGURE 7B

IV. LIMITATIONS OF MRCP

In MRCP, like any MR study, the general contraindications to MR imaging apply. However, it has been reported that the rate of MRCP failure due to contraindications and claustrophobia is overall less than that of ERCP. Guibaud²⁴ reported rates of unsuccessful and inadequate MRCPs of 4 and 5%, respectively. Conversely, ERCP accounted for 8 and 6% of cases, respectively. Furthermore, MRCP can be performed in patients with altered anatomy such as Billroth II anastomosis, duodenal stenosis, or choledochojejunostomy.

The signal continuity in the bile ducts can be interrupted by the presence of surgical clips, pneumobilia, and motion artifacts secondary to the duodenal peristalsis. Thrombi, protein plaques, or calculi can also account for this. It can be easily assumed, therefore, that a signal void within the bile ducts cannot be specific for calculi. Nevertheless, the same problem can also be encountered with ERCP in which often the common bile duct stones from air bubbles cannot be easily differentiated. The differential diagnosis of pneumobilia and choledocholithiasis can be made by carefully observing axial MR images in which air bubbles will float anterior to bile, whereas calculi will lie in the dependent portion of the bile duct.

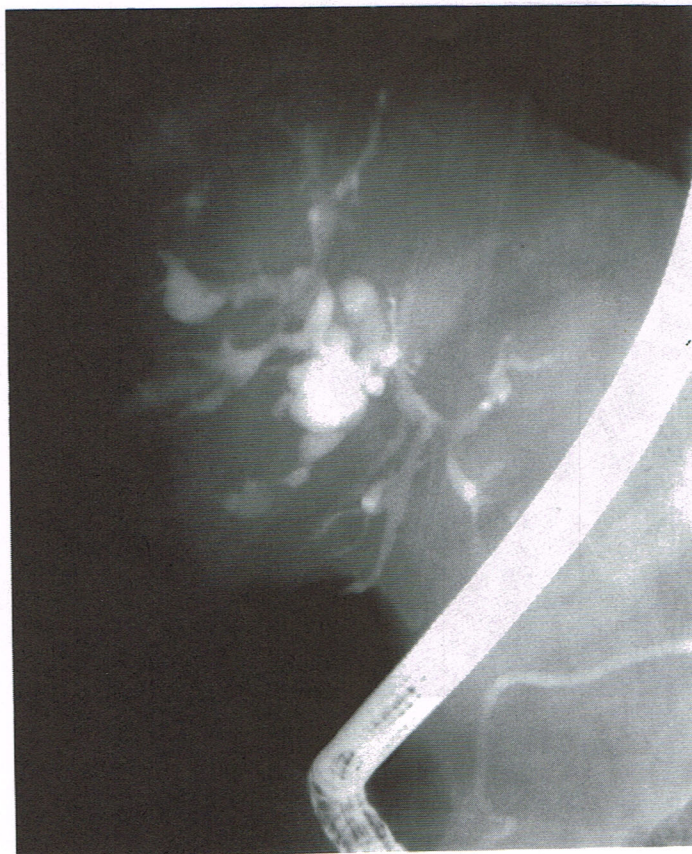


FIGURE 7C

Duct calibers are usually underestimated in ERCP and a discrepancy between the calibers of the duct measured at ERCP and MRCP is a known phenomenon. Two factors may account for this. First, volume averaging that occurs at the periphery of the ducts, and, second, overdistention or even under filling of the ducts during ERCP. However, during MRCP, the ducts are examined in their physiologic stationary and neutral state.

The spatial resolution of MRCP is very limited compared with that ERCP, at least at its present stage. This results in inability of MRCP to provide detailed anatomic morphology of a stricture and also bile duct stones that are less than 3 mm in diameter. By the same token, minimal narrowing of pancreatic duct side branches cannot be routinely visualized unless dilated. MRCP offers the advantage of being an MR technique that requires no special technical or additional skills. However, ERCP not only requires an endoscopist but is done under sedation and is highly operator dependent. The interobserver agreement in MRCP has been reported to be very high.²⁴

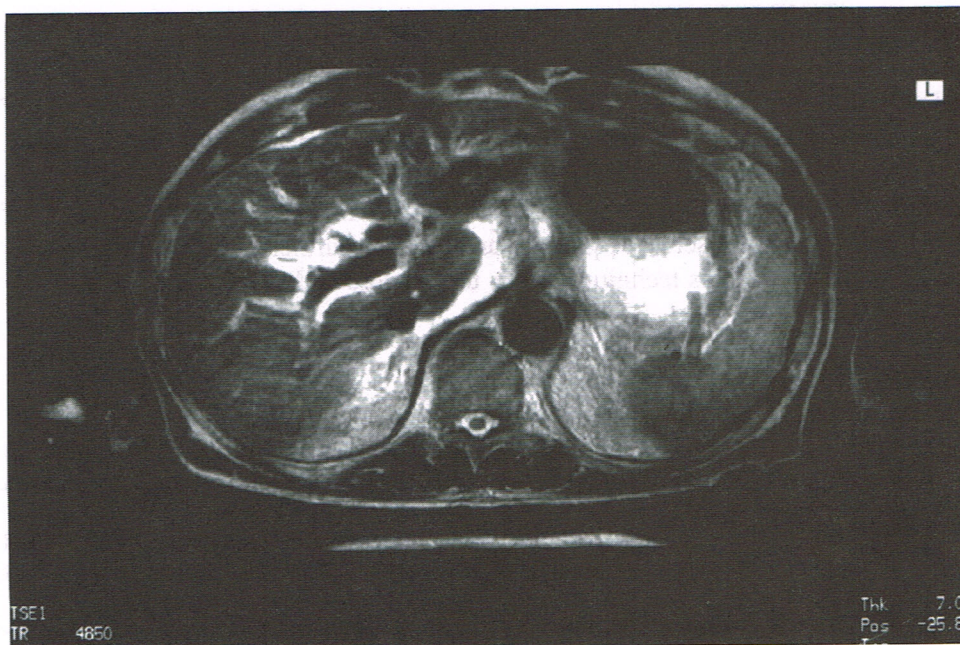


FIGURE 8. Pitfall. This 73-year-old man has gastric carcinoma with lymphadenopathy at the porta hepatis. Axial MIP of the FSE T2 images demonstrates extensive increased signal (arrows) surrounding the intrahepatic portal venous system. This represents periportal edema and mimics intrahepatic duct dilatation that was absent in this patient.

One of the major advantages of ERCP compared with MRCP is that ERCP provides the additional option of therapeutic intervention during the same examination session. On the other hand, the major advantage of MRCP is simultaneous evaluation of other neighboring anatomic structures, such as liver, porta hepatis, pancreas, and retroperitoneum.

V. CONCLUSION

Our work and those in the literature indicate that MRCP is an evolving and clinically useful technique. The location of an obstruction can easily be demonstrated on the MIP images. However, the source images should always be routinely evaluated prior to establishing the diagnosis. Patients unable to undergo more conventional invasive studies such as PTC or ERCP, those with altered gastroduodenal anatomy, and patients who had unsuccessful results from the above examinations are more likely to benefit from MRCP.

Breath hold sequences are preferred over non-breath hold, as the latter can be degraded by motion artifacts. The preliminary results are promising; however, the

technique needs continuous improvement in order to further increase the spatial resolution and signal-to-noise ratio. Certain pitfalls and false-negative as well as false-positive diagnoses are possible. These are more often encountered in cases of small common bile duct stones that are either missed or misinterpreted as tumor.

Overall, it cannot be predicted yet whether MRCP will substitute ERCP on a routine basis. This will depend on improvements in the diagnostic accuracy of MRCP after a longer series of patients are studied. Furthermore, a cost-effectiveness assessment of this technique needs to be addressed.

REFERENCES

1. **Ferrucci, J. T.**, MR cholangiopancreatography in radiology of the liver, biliary tract and pancreas. Categorical Course Syllabus, Freeny, P. C., Ed., ARRS 96th Annual Meeting, San Diego, CA, 1996.
2. **Wallner, B. K., Schumacher, K. A., Weidenmaier, W., and Friedrich, J. M.**, Dilated biliary tract: evaluation with MR cholangiography with a T2-weighted contrast-enhanced fast sequence, *Radiology*, 181, 805, 1991.
3. **Morimoto, K., Shimoi, M., Shirakawa, T. et al.**, Biliary obstruction: evaluation with three-dimensional MR cholangiography, *Radiology*, 183, 578, 1992.
4. **Ishizeki, Y., Wakayama, T., Okada, Y., and Kobayashi, T.**, Magnetic resonance cholangiography for evaluation of obstructive jaundice, *Am. J. Gastroenterol.*, 12, 2072, 1993.
5. **Hall-Craggs, M., Allen, C., Owens, C. et al.**, MR cholangiography: clinical evaluation in 40 cases, *Radiology*, 189, 423, 1993.
6. **Takehara, Y., Ichijo, K., Tooyama, N. et al.**, Breath-hold MR cholangiopancreatography with a long-echo-train fast spin-echo sequence and a surface coil in chronic pancreatitis, *Radiology*, 192, 73, 1994.
7. **Outwater, E. K.**, MR cholangiography with a fast spin-echo sequence (Abstr.), *JMRI*, 3(P), 131, 1993.
8. **Barish, M. A., Yucek, K. E., Soto, J. A. et al.**, MR cholangiopancreatography: efficacy of three-dimensional turbo spin-echo technique, *AJR*, 165, 295, 1995.
9. **Soto, J. A., Barish, M. A., Yucel, K. E. et al.**, Pancreatic duct: MR cholangiopancreatography with a three-dimensional fast spin-echo technique, *Radiology*, 196, 459, 1995.
10. **Meakem, T. J., III and Schnall, M. D.**, Magnetic resonance cholangiography, *Gastroenterol. Clin. N.A.*, 24(2), 221, 1995.
11. **Miyazaki, T., Yamashita, Y., Tsuchigame, T., Yamamoto, H., Urata J., and Takahashi, M.**, MR cholangiopancreatography using HASTE (half-fourier acquisition single shot turbo spin-echo) sequences, *AJR*, 166, 1297, 1996.
12. **Reinhold, C., Guibaud, L., Genin, G., and Bret, P. M.**, MR cholangiopancreatography: comparison between two-dimensional fast spin-echo and three-dimensional gradient-echo pulse sequences, *J. Magn. Reson. Imag.*, 4, 379, 1995.
13. **Meakem, T. J., Holland, G. A., McDermott, G. M. et al.**, Fast spin echo multicoil magnetic resonance cholangiography, initial experience (Abstr.), in Proceedings of the Society of Magnetic Resonance in Medicine, Berkeley, California: Society of Magnetic Resonance in Medicine, 1993, 47.
14. **Reinhold, C. and Bret, P. M.**, Current status of MR cholangiopancreatography, *AJR*, 166, 1285, 1996.
15. **MacCaulay, S. E., Schulte, S. J., Sekijima, J. H. et al.**, Evaluation of a non-breath-hold MR cholangiography technique, *Radiology*, 196, 227, 1995.

16. **Bret, P. M., Reinhold, C., Taourel, P. et al.**, Pancreas divisum: evaluation with MR cholangiopancreatography, *Radiology*, 199, 99, 1996.
17. **Reuther G., Kiefer B., and Tuchmann A.**, Cholangiography before biliary surgery: single-shot MR cholangiography vs. intravenous cholangiography, *Radiology*, 198, 561, 1996.
18. **Lee M.-G., Lee H.-J., and Kim M. H. et al.**, Extrahepatic biliary diseases: 3D MR cholangiopancreatography compared with endoscopic retrograde cholangiopancreatography, *Radiology*, 202, 663, 1997.
19. **Panasen, P., Partanen, K., Pikkarainen, P. et al.**, Ultrasonography CT and ERCP in the diagnosis of choledochal stones, *Acta Radiol.*, 33, 53, 1992.
20. **Stott, M. A., Farrand, P. A., Guyer, P. B. et al.**, Ultrasound of the common bile duct in patients undergoing cholecystectomy, *J. Clin. Ultrasound*, 19, 73, 1991.
21. **Todua, F. L., Karmazanovskii, G. G., and Vikhorev, A. V.**, Computerized tomography of the mechanical jaundice in the involvement of the distal region of the common bile duct, *Vestn. Rentgenol. Radiol.*, 2, 15, 1991.
22. **Guibaud, L., Bret, P. M., Reinhold, C., Atri, M., and Barkun, A. N.**, Diagnosis of choledocholithiasis: value of MR cholangiography, *AJR*, 163, 847, 1994.
23. **Soto, J. A., Barish, M. A., Yucel, K. E. et al.**, Magnetic resonance cholangiography: comparison with endoscopic retrograde cholangiopancreatography, *Gastroenterology*, 110, 589, 1996.
24. **Guibaud, L., Bret, P. M., Reinhold, C. et al.**, Bile duct obstruction and choledocholithiasis: diagnosis with MR cholangiopancreatography, *Radiology*, 197, 109, 1995.
25. **Taourel, P., Bret, P., Reinhold, C. et al.**, MR cholangiography of anatomical variants of the biliary tree, *Radiology*, in press.
26. **Sherman, S. and Lehmen, G. A.**, ERCP and endoscopic sphincterotomy-induced pancreatitis, *Pancreas*, 6, 350, 1991.
27. **Todani, T., Watanabe, Y., Navusue, M. et al.**, Congenital bile duct cyst: classification, operative procedures and review of 37 cases, including cancer arising from choledochal cyst, *Am. J. Surg.*, 134(2), 263, 1977.